CHALLENGES IN EUROPEAN AEROSPACE
5TH CEAS AIR & SPACE CONFERENCE

CEAS

Computation of Thermodynamic Cycle for Novel Detonation Aircraft Engine

Cleopatra F. Cuciumita
COMOTI Romanian Research and Development Institute for Gas Turbines
Senior Researcher
220 D Iuliu Maniu Bd., sector 6, Postal code 061126, Bucharest, Romania
E-mail: cleopatra.cuciumita@comoti.ro
Ionut Porumbel (COMOTI Romanian Research and Development Institute for Gas Turbines)

ABSTRACT

The paper presents the thermodynamic cycle for a novel detonation based, aircraft engine. First, an overview of the existing models is presented, introducing the most common detonation models in the literature: the Humphrey cycle, the Zeldovitch - Neumann - van Doring cycle, and the Fickett - Jacobs cycle. Algorithms for determining the thermodynamic cycles for the selected three detonation models are presented, and numerical results for a case study involving a detonation based, aircraft engine are provided. Finally, the theoretical cycle efficiency, the useful work and the cycle specific heat for the studied engine are also determined.

NOMENCLATURE

Latin
c - Specific heat
h - Enthalpy
q - Heat release
p - Pressure
v - Specific volume
w - Specific work
M - Mass flow rate
R - Gas constant
T - Temperature
X - Mole fractions
Y - Mass fractions

Greek
δ_n - Nozzle pressure ratio
η - Efficiency
π_c - Compressor pressure ratio
σ - Heat losses
φ - Kinetic energy losses

Superscripts
H - Humphrey detonation cycle
FJ - Fickett - Jacobs detonation cycle
ZND - Zeldovich - von Neumann – Doring detonation cycle

Subscripts
1 - Compressor inlet (stagnation parameters)
2 - Compressor outlet
3 - Combustor outlet
5 - Nozzle outler
atm – Atmospheric
c – Compressor
cb - Combustion chamber
f - Formation
g - Gas (combustion gas)
id - Ideal
n - Nozzle
p - Constant pressure
v- Constant volume

1 PULSE DETONATION ENGINE TECHNOLOGY

The rising interest in the detonation engines originates in the higher efficiency, which can be reached by constant-volume combustion. Compared to a constant pressure process, pressure-gain combustors allow reaching the same exit temperature at higher pressure, leading to higher cycle efficiency.
Detonation differs from other combustion processes in the way in which the physical phenomenon evolves. The detonation is formed by a leading shock wave which propagates in the explosive mixture. The propagating shock wave triggers the chemical reactions and thus, the heat release. In a Pulse Detonation Engine (PDE), detonation is generated in a tube (detonation combustion chamber). The detonation wave rapidly propagates inside the chamber resulting in a nearly constant-volume heat

addition process that determines a high pressure in the combustor and provides the thrust. The interest of the scientific community on the research and development of pulse detonation engine has grown in the last few years, due to the potential gain in specific power. Very rapid species and energy conversion happens during detonation. This rapid conversion rate, which could be 2 or 3 orders of magnitude faster than in a flame, can lead to several advantages for propulsion application. Due to the rapidity of the process, the equilibrium state in pressure cannot be reached and the process thermodynamically behaves as a constant volume process. The latter is more efficient than a constant pressure process, typical of conventional propulsion systems.

The three principal cycles considered in the detonation modeling and in the detonation performance estimation are: the Humphrey, the Fickett-Jacobs (FJ) and the Zeldovich-von Neumann-Doring (ZND) cycle. In Figure 1, Figure 2 and Figure 3 the cycles are plotted in the p-v and T-s diagrams [1]. The Humphrey cycle is the simplest one for the PDE engine cycle modeling. It assumes that the compression process is isochoric, followed by an isentropic expansion and an isobaric process to close the cycle. In the Humphrey cycle, the post-compression is not represented by the Chapman-Jouguet (CJ) conditions, thus the performance of the PDE are under predicted. The FJ cycle consist of a compression and heat release, from point (1) to point (3CJ) in Figure 2 The heat release is considered to be an equilibrium process strictly one-dimensional. In this case, the process can be assumed equal to the Rayleigh heating. In other words, the tangent from point (1) to point (2CJ) is represented by the Rayleigh heating curve. The process occurring from point (2CJ) to (3CJ) consists in the isentropic expansion, followed by the isobaric process to close the cycle.

The most accurate model for a detonation cycle is the Zeldovich-von Neumann-Doering (ZND). The detonation wave consists in a normal shock wave progressing into the undisturbed fuel-oxidiser mixture, followed by release of heat in a constant-area region (Rayleigh flow). The strength of the leading shock wave is uniquely determined by the initial conditions and the amount of heat added. The entire process is constrained by the Chapman-Jouguet condition. The latter implies that, after the heat addition-area, the local Mach number is equal to 1. The heat addition region is followed by a complex flow region, where the non-steady Taylor expansion waves take place. Figure 4 shows the phases of a PDE engine [1].

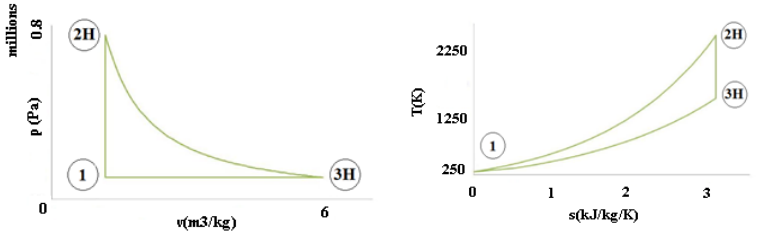

Figure 1: - Humphrey cycle in the p-v and T-s planes [1]

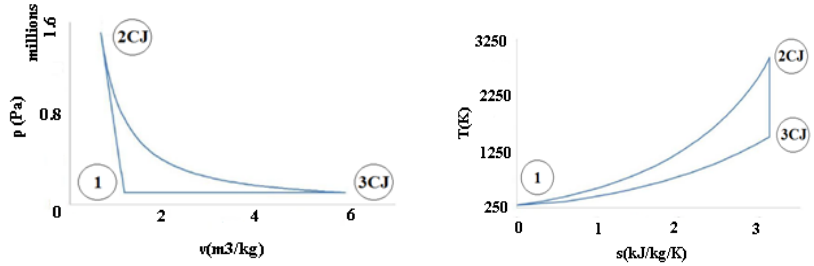

Figure 2: – Fickett-Jacobs cycle in the p-v and T-s planes [1]

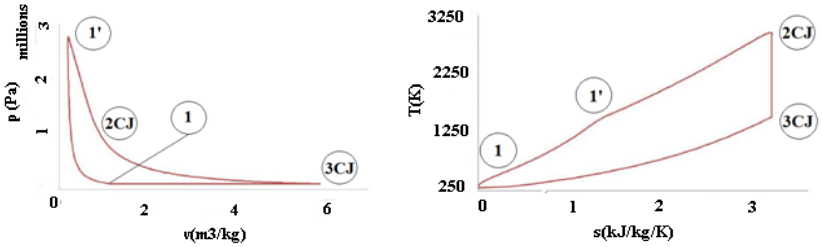

Figure 3 – ZND cycle in the p-v and T-s planes [1]

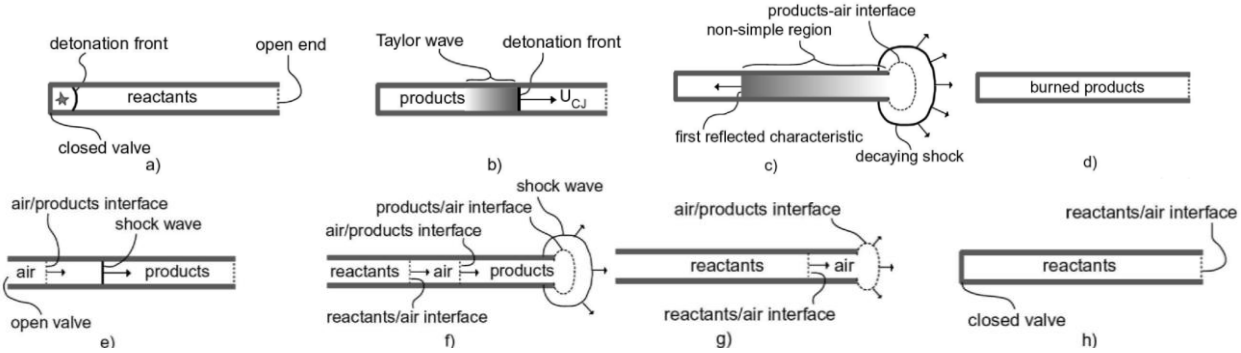

Figure 4: –PDE cycle phases [1]

Considering the ideal PDE cycle modeled with the ZND assumptions, one can compare the efficiency of the typical constant pressure-based combustion cycle (Brayton) to the efficiency of the ideal Humphrey and the ideal PDE. In Figure 5, the thermal efficiency is plotted in function of the ratio between the pressure at the end of the adiabatic isentropic compression and the free stream static pressure. The three cycles are compared considering heat addition , where is defined as follows:

$$\tilde{q} = \frac{q_{supp}}{c_p T_0} = \frac{f h_{PR}}{c_p T_0} \tag{1}$$

Where is the mass fuel-air ratio and is the lower heating value of the fuel.

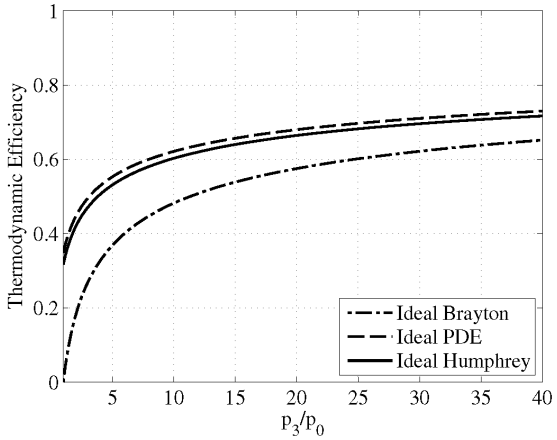

Figure 5 –Thermal efficiency of Brayton, Humphrey and PDE ideal cycles

It is important to say that the efficiency of the cycle component (compressor, expander, combustion chamber) affects the cycle efficiency, yielding to lower thermodynamic efficiency for the PDE with respect to the Brayton for high values of [2].

2 INPUT DATA, CONSTANTS AND STANDARD PARAMETERS

The case study selected for the present paper is defined by the following input data [3]:

Table 1: Input data for the case study

Parameter	**Symbol**	**Value**	**Measurement Unit**
Engine compressor total to static pressure ratio	π_c	6	-
Gas constant for air	R	287.3	J/kg/K
Gas constant for burned gas	R_q	288.4	J/kg/K
Specific heat ratio for air	γ	1.4	-
Specific heat ratio for burned gas	γ_q	1.33	-
Specific heat at constant pressure ratio for air	c_p	1005	J/kg
Specific heat at constant pressure ratio for burned gases	c_{pq}	1165	J/kg
Standard atmospheric conditions: pressure, temperature, entropy	P_{atm}, T_{atm}, s_{atm}	101330 288 660.122	Pa K J/kg/K
Compressor efficiency for centrifugal compressors	H_c	0.85	-
Combustor heat losses	σ_{cb}	0.9	-
Exhaust nozzle kinetic energy losses	φ_n	0.95	-

The case study engine is fuelled by a stoechiometric mixture of air and acetylene. The mixture properties are provided in Table 2.

Table 2: Fuel mixture properties

	Reactants			
Species	C_2H_2	O_2	N_2	Total
Moles	2	5	18.810	25.810
MW	26	32	28	86
X	0.07749	0.19373	0.72878	1
Y	0.07040	0.21660	0.71300	1
h_f [kJ/kg]	8721.077	0	0	8721.077
q [J/kg]	613938.6	0	0	613938.6
	Products			
Species	CO_2	H_2O	N_2	Total
Moles	4	2	18.810	24.810
MW	44	18	28	90
X	0.16123	0.08061	0.75816	1
Y	0.23827	0.04873	0.71300	1
h_f [kJ/kg]	-8944.227	-13435.833	0	-22380.061
q [J/kg]	-2131115.5	-654815.0	0	-2785931.5

Since the specific heat at constant pressure is defined as a mixture average, the sensible enthalpies of the species in the mixture cancel out when determining the heat of reaction for the acetylene combustion, so they were neglected. The data in Table 1 comes from reference [4].
Based on the data in Table 2, the heat of combustion is:

$$q_{id} = -3399869.134\ J/kg \tag{2}$$

3 IDEAL THERMODYNAMIC CYCLE

3.1 Initial conditions

State 1id, the compressor inlet, also coincides with the engine inlet, as the TIDE engine is not equipped with any air intake ducting. Thus, state 1id will correspond to air at atmospheric conditions under which the engine operates.
For the present work, standard atmospheric conditions at sea level and at zero flight velocity are assumed for the starting point of the TIDE engine thermodynamic cycle. Certainly, a real engine is expected to operate under a vast region of intake conditions, due to various altitudes, flight velocities, or specific atmospheric conditions. However, the resulting thermodynamic cycles are outside the scope of the present work. Furthermore, once the algorithm for computing the thermodynamic cycle is established, as per this work, applying various inlet conditions becomes straight forward.
Thus, p_{1id}, T_{1id} and s_{1id} are the standard atmospheric conditions defined earlier.
The specific volume is given by [5]:

$$v = \frac{RT}{p} \tag{3}$$

Equation (3) can be applied to determine v_{1id}.
The enthalpy is determined using [3]:

$$h = c_p T \tag{4}$$

Equation (4) can be applied to determine h_{1id}.

3.2 Ideal compression

The whole paper should be formatted as a single column.
State 2id, the compressor outlet, also coincides with the combustor inlet. The air compression is assumed adiabatic (no heat losses in the engine compressor). State 2id, the ideal compression, is reached from state 1id through an isentropic adiabatic compression. Since path 1id - 2id is isentropic:

$$s_{2id} = s_{1id} \tag{5}$$

The pressure at state 2id is determined by:

$$p_{2id} = p_1 \pi_c \tag{6}$$

The entropy at a given temperature and pressure, can be determined from the entropy at a reference state 0 by [5]:

$$s = s_0 + c_p \ln\left(\frac{T}{T_0}\right) - R\ln\left(\frac{p}{p_0}\right) \tag{7}$$

Applying Equation (7) for state 2id, and using state 1id as reference, the temperature T_{2id} can be determined as:

$$T_{2id} = T_{1id}\left(\frac{p}{p_0}\right)^{\frac{R}{c_p}} \tag{8}$$

Next, knowing T_{2id}, Equation (4) can be applied to determine the enthalpy h_{2id}.
The specific volume v_{2id} can be determined using Equation (3) for the conditions at state 2id.

3.3 Ideal detonation

State 3id corresponds to a point immediately downstream of the detonation wave. It is important to note that state 3id does not have a fixed geometrical location throughout the detonation cycle, but travels through the combustor together with the detonation wave. During the detonation process, the system is temporarily non-uniform and, therefore, the line representing the 2id – 3id evolution in Figures 1 - 2 is not an actual thermodynamic path, but merely a conventional representation of the non-equilibrium detonation process [6]. The heat of combustion is given by Equation (2). For the PDC evolution, three detonation models will be considered: the Humphrey cycle [8], the Fickett - Jacobs cycle [9, 10], and the Zeldovitch - Neumann - van Doring cycle [11]. It is important to note that, contrary to classic thermodynamic cycles, the detonation cycle is not a succession of equilibrium states.

3.3.1 The Humphrey cycle

The Humphrey cycle path includes state 3^Hid. The path 2 - 3^H_{id} is assumed as a constant volume heating up to a temperature corresponding to the heat release given by Equation (4).
For a constant volume evolution:

$$v_{3id}^H = v_2 \tag{9}$$

The heat release by chemical reaction can be written, in the ideal case, for a constant volume process:

$$q_{id} = c_{vg}(T_{3id}^H - T_2) \tag{10}$$

The specific heat at constant pressure and at constant volume and the temperature in state 3^Hid can be determined as [5]:

$$c_{vg} = c_{pg} - R_g \tag{11}$$

Finally, by combining Equations (10) – (11):

$$T_{3id}^{H} = \frac{q_{id}}{c_v} + T_2 \tag{12}$$

The pressure is determined using Equation (3) for state 3^{H}id.
The enthalpy h^{H}_{3id} is found by applying Equation (4) for temperature T^{H}_{3id} for burned gas.
Similarly, the entropy at state 3^{H}id is calculated by using Equation (7) with state 2id as the reference state.

3.3.2 The Fickett - Jacobs cycle

The Fickett - Jacobs cycle path includes state 3^{F}id. The approach assumes that the detonation can be modeled as a compression with heat addition process. Under the Chapman - Jouguet theory [12, 13], the heat release through detonation is assumed instantaneous, and the process is identical to a Rayleigh heating and the process can be regarded as being in local thermodynamic equilibrium [14]. Thus, in the p-v plane, the point 3^{F}id is found at the intersection of the reactive Hougoniot curve corresponding to the acetylene adiabatic flame temperature with the tangent from point 2id to the same reactive Hougoniot curve [12], also known as the Rayleigh line [4].
The general reactive Hougoniot curve based on the state 2id parameters and on the heat release given by Equation (2) is [15]:

$$\left(\frac{p}{p_{2id}} + \frac{\gamma_g - 1}{\gamma_g + 1}\right) + \left(\frac{v}{v_{2id}} - \frac{\gamma_g - 1}{\gamma_g + 1}\right) = 1 - \left(\frac{\gamma_g - 1}{\gamma_g + 1}\right)^2 + 2\frac{\gamma_g - 1}{\gamma_g + 1}\frac{q_{id}}{p_{2id}v_{2id}} \tag{13}$$

A line passing through point 2id in the p-v plane can be written as:

$$\frac{p}{p_{2id}} = m\left(\frac{v}{v_{2id}} - 1\right) + 1 \tag{14}$$

where m is the slope of the Raighleigh line.
By substituting Equation (14) into Equation (13), a second order equation in v is obtained. To impose the condition that the line defined by Equation (14) is a Rayleigh line, i.e. tangent to the Hugoniot curve (13), the discriminant of the previously mentioned second order equation must be zero. Under this condition, another second order equation in m is obtained:

$$\left(\frac{\gamma_g - 1}{\gamma_g + 1} - 1\right)^2 m^2 - 2\left[\left(\frac{\gamma_g - 1}{\gamma_g + 1}\right)^2 - 4\frac{\gamma_g - 1}{\gamma_g + 1}\frac{q_{id}}{p_{2id}v_{2id}} - 1\right] + \left(\frac{\gamma_g - 1}{\gamma_g + 1} - 1\right)^2 = 0 \tag{15}$$

Solving Equation (15), the slope of the Rayleigh line is known. Since the upper Chapman – Jouguet is sought, the solution with the negative sign in front of the discriminant square root solution will be selected. Next, the specific volume in state 3^Fid can be obtained from the zero discriminant second order equation as:

$$v_{3id}^F = \left[\frac{(m-1)}{2m}\left(\frac{\gamma_g - 1}{\gamma_g + 1} + 1\right)\right] v_{2id} \tag{16}$$

The pressure in state 3^Fid can now be determined by substituting Equation (16) in Equation (14):

$$p_{3id}^F = \left[m\left(\frac{v_{3id}^F}{v_{2id}} - 1\right) + 1\right] p_{2id} \tag{17}$$

The temperature can be determined by applying the equation of state (3) for the conditions in state 3^Fid. With the known temperature, the enthalpy h^F_{3id} is found by applying Equation (4) for burned gas. Similarly, the entropy is calculated by using Equation (7) with state 2id as the reference state.

3.3.2 The Zeldovich – von Neumann - Doring cycle

The Zeldovich – von Neumann - Doring cycle path includes states $3'^Z$id and $3'^Z$id. The ZND model assumes the detonation is composed of an initial non-reactive shock wave, along the so-called inert Hugoniot and bringing the thermodynamic system is state $3'^Z$id, immediately followed by heat release along a Rayleigh line [14], bringing the system in state $3'^Z$id.
The point in the *p-v* plane corresponding to state $3'^Z$id can be found at the intersection between the inert Hugoniot and the Rayleigh line. As the Rayleigh line is unique for given initial conditions and heat release, it is defined by Equation (14) as well. The inert Hugoniot, in its turn, can be defined by annulling the heat release term in Equation (13):

$$\left(\frac{p}{p_{2id}} + \frac{\gamma_g - 1}{\gamma_g + 1}\right)\left(\frac{v}{v_{2id}} - \frac{\gamma_g - 1}{\gamma_g + 1}\right) = 1 - \left(\frac{\gamma_g - 1}{\gamma_g + 1}\right)^2 \tag{18}$$

Similarly to the FJ cycle, by substituting Equation (14) into Equation (18), a second order equation in v can be obtained:

$$m(v_{3'id}^Z)^2 + \left(1 - m - m\frac{\gamma_g - 1}{\gamma_g + 1} + \frac{\gamma_g - 1}{\gamma_g + 1}\right) v_{3'id}^Z + m\frac{\gamma_g - 1}{\gamma_g + 1} - \frac{\gamma_g - 1}{\gamma_g + 1} - 1 = 0 \tag{19}$$

Equation (19) provides two solutions, corresponding to the two intersection points. One point represents state 2id, while the other, whose volume is given by the solution of Equation (19) with the positive sign in front of the discriminant square root, is the sought point.

Next, the pressure is determined by substituting the previously determined specific volume into Equation (14).
As before, the temperature can be determined by applying the equation of state (3) for the conditions in state $3''^{Z}$id. With the known temperature, the enthalpy $h^{Z}_{3''id}$ is found by applying Equation (4) for burned gas. Similarly, the entropy s^{Z}_{3id} is calculated by using Equation (7) for air.
Since both states 3^{F}id and 3^{Z}id correspond to the upper Chapman – Jouguet point [4], they must be identical for the same cycle parameters.

3.4 Ideal Expansion

State 4id represents the engine nozzle outlet. The air expansion is assumed adiabatic (no heat losses in the engine combustor and nozzle). State 4id, the ideal expansion, is reached from either of the states 3id through an isentropic adiabatic expansion. Since the parameters characterizing state 3id are different for each of the three considered detonation models, three different parameters sets characterizing state 4id will be obtained. However, the algorithm for determining them is the same, only the initial state 3id being different.
As path 3id - 4id is isentropic:

$$s_{4id} = s_{3id} \tag{20}$$

The expansion is assumed to be complete, down to the atmospheric pressure:

$$p_{4id} = p_{atm} \tag{21}$$

Applying Equation (8) for burned gas, the temperature T_{4id} can be determined. Next, knowing T_{4id}, Equation (4) can be applied to determine the enthalpy h_{4id} with the coefficients for burned gas.
The specific volume v_{4id} can be determined using Equation (3) for the conditions at state 4id.

3.5 Ideal Cycle Closure

The ideal cycle is closed by a fictitious isobar that connects states 4id and 1.

3.6 Ideal Cycle Results

The numerical results of the previously presented algorithm applied for the case study studied in this paper are presented in Table 3, and Figure 6.

Table 3: The ideal cycle

State	P [Pa]	T [K]	v [m³ / kg]	h [J/kg]	s [J/kg K]	w or q [J/kg]	m
1	101330	288.00	0.81656	289440.000	6660.122	0.000	-
2id	607980	480.67	0.22714	483068.980	6660.122	193628.980	-
3^{H}id	5534858	4359.14	0.22714	5078396.133	8591.799	-822768.278	-
3^{F}id	10822706	4985.69	0.13286	5808323.610	8554.859	-822768.278	-40.47654
$3''^{Z}$id	21037432	2824.72	0.03858	2838843.533	7421.803	0.000	-40.47654
3^{Z}id	10822706	4985.69	0.13286	5808323.610	8554.859	-822768.278	-40.47654

$4^H id$	101330	1619.23	4.60857	1886403.871	8591.799	-3191992.262	-
$4^F id$	101330	1568.69	4.46473	1827527.902	8554.859	-3980795.708	-
$4^Z id$	101330	1568.69	4.46473	1827527.902	8554.859	-3980795.708	-

In order to determine the proper temperature, enthalpy and the entropy between state 2id and each of the states 3id, as well as along the final isobars 4id - 1, it is important to note that the working fluid composition changes during the evolutions from air to burned gas, and from burned gas to air, respectively, which affects both the gas constant and the curve fit coefficients for enthalpy and entropy at one bar.
To circumvent this problem, a progress variable, φ, was introduced, and the affected variables along the gas composition changing evolutions 2id - 3id (or, rather, 3'id – 3id in the ZND case), and 4id – 1 are determined as:

$$a = a_{air}(1-\phi) + a_g\phi \tag{22}$$

where a is temperature, enthalpy, or entropy, and the progress variable Φ, varies between 0 (for states 3id and 4id) and 1 (for states 2id and 1).

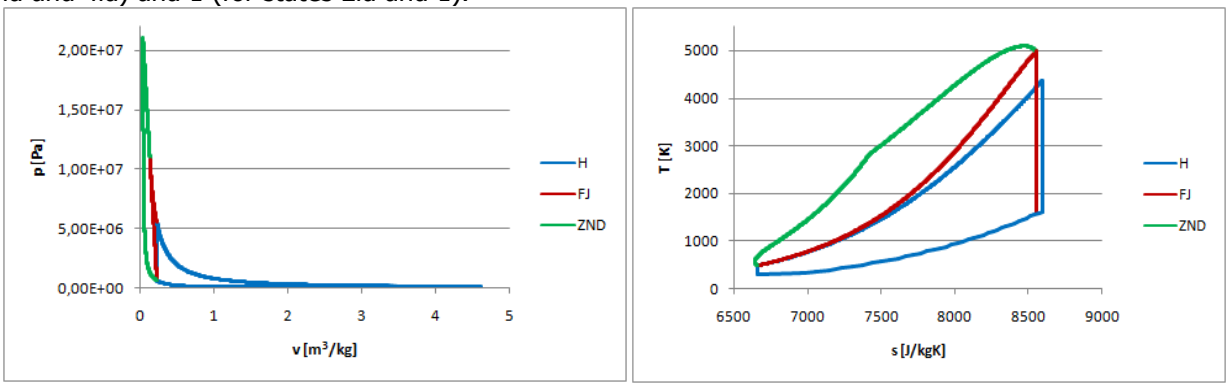

Figure 6: p-v diagram of the ideal cycle (left), T-s diagram of the ideal cycle (right)

4 REAL THERMODYNAMIC CYCLE

4.1 Initial Conditions

The real initial conditions are identical to the ideal initial conditions. State 1 will correspond to air at atmospheric conditions under which the engine operates.

4.2 Real Compression

State 2, the real compression is reached, from state 1, through a non-isentropic adiabatic compression. For state 2, the path 1 - 2 is still adiabatic, but not isentropic anymore. Instead of the ideal work, defined as [3]:

$$w_{c,id} = h_{2id} - h_1 \tag{23}$$

the real compressor work will be used to bring the air in state 2id:

$$w_c = h_2 - h_1 = \frac{w_{c,id}}{\eta_c} \tag{24}$$

By combining Equations (23) and (24), the state 2 enthalpy is:

$$h_2 = h_1 + \frac{h_{2id} - h_1}{\eta_c} \tag{25}$$

Applying Equation (25), and using Equation (4) for state 2, for air, the temperature T_2 can be determined.
The pressure is the same in states 2id and 2:

$$h_2 = p_{2id} \tag{26}$$

The specific volume v_2 can be determined using Equation (3) for the conditions at state 2.
The entropy at state 2 can be determined using Equation (7) for air, with state 1 as the reference state.

4.3 Real Detonation

State 3 represented the real detonation. As for the ideal case, state 3 does not have a fixed geometrical location throughout the detonation cycle, but travels through the combustor together with the detonation wave, and the line representing the 2 – 3 evolution in Figures 3 - 4 is not an actual thermodynamic path, but merely a conventional representation of the non-equilibrium detonation process [14]. For the real case, heat losses due to heat transfer through the combustion walls and incomplete combustion are considered, so the heat released by the detonation process is:

$$q = q_{2id}\sigma_{ca} \tag{27}$$

As before, the Humphrey cycle, the Fickett - Jacobs cycle, and the Zeldovitch - Neumann - van Doring cycles will be considered. The algorithm for all the three models remains identical with the ideal case, but with the heat release given by Equation (27) instead of Equation (2).

4.4 Real Expansion

State 4 represents the engine nozzle outlet. The air expansion is assumed adiabatic (no heat losses in the engine combustor and nozzle). State 4, the real expansion, is reached from either of the states 3 through a non-isentropic adiabatic expansion. Since the parameters characterizing state 3 are different for each of the three considered detonation models, three different parameters sets characterizing state 4 will be obtained. However, the algorithm for determining them is the same, only the initial state 3 being different.
The ideal expansion work between states 3 and 4 is expressed as [5]:

$$w_{n,id} = h_3\left(\delta_n^{\frac{\gamma_g - 1}{\gamma_g}} - 1\right) \tag{28}$$

where the nozzle pressure ratio is defined as:

$$\delta_n = \frac{p_4}{p_3} \tag{29}$$

The real expansion work is determined by taking into account the kinetic energy losses in the nozzle:

$$w_n = w_{n,id}\phi_n \tag{30}$$

Then, the enthalpy at state 4 is:

$$h_4 = h_3 + w_n \tag{31}$$

Applying Equation (4) for burned gas, the temperature T_4 can be determined. As for the ideal case, the expansion is assumed to be complete, down to the atmospheric pressure:

$$p_4 = p_{atm} \tag{32}$$

The specific volume v_4 can now be determined using Equation (3) for the conditions at state 4.
Finally, knowing T_4, Equation (7) for burned gas can be applied to determine the entropy s_4, using states 3 as the reference states.

4.5 Real Cycle Closure

The real cycle is closed by a fictitious isobar that connects states 4 and 1.

4.6 Real Cycle Results

The numerical results of the previously presented algorithm applied for this case study input data are presented in Table 4, and Figure 7.

Table 4: The real cycle

State	p [Pa]	T [K]	v [m^3 / kg]	h [J/kg]	s [J/kg K]	w or q [J/kg]	m
1	101330	288.00	0.81656	289440.000	6660.122	0.000	-
2	607980	514.67	0.24320	517238.800	6728.809	227798.800	-
3^H	4759884	4013.95	0.24320	4676257.175	8528.257	-3059882.220	-
3^F	9245427	4579.65	0.14286	5335292.004	8490.386	-3059882.220	-34.43183
3^Z	17882873	2635.86	0.04251	2649043.053	7398.933	0.000	-34.43183
3^Z	9245427	4579.65	0.14286	5335292.004	8232.754	-3059882.220	-34.43183

4^H	101330	1593.76	4.53607	1856728.797	8562.391	-2819528.379	-
4^F	101330	1556.11	4.42893	1812873.107	8534.544	-3522418.896	-
4^Z	101330	1556.11	4.42893	1812873.107	8534.544	-3522418.896	-

The variation of the gas composition between states 2 and 3, respectively between states 4 and 1, was handled in the same way as for the ideal cycle case.

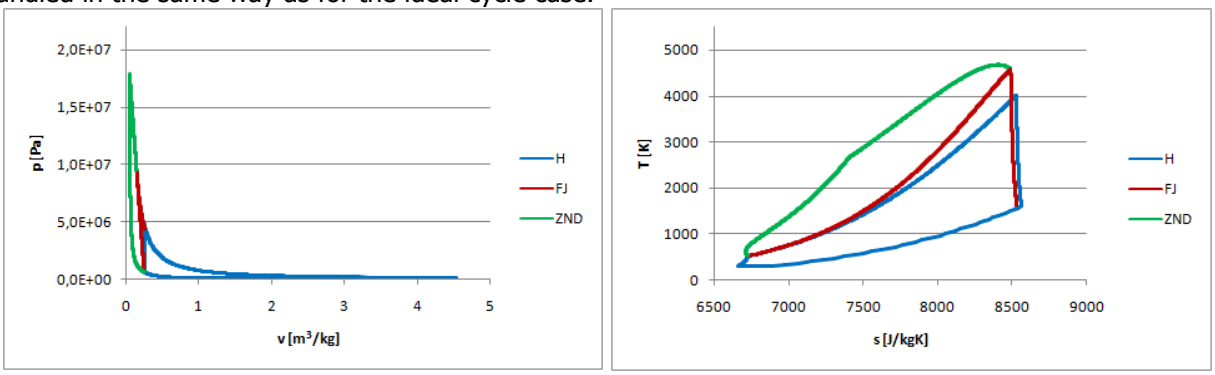

Figure 7: p-v diagram of the real cycle (left), T-s diagram of the real cycle (right)

5 WORK AND EFFICIENCY

The TIDE cycle net specific work can be determined as [14]:

$$w_{cycle} = \oint p dv \tag{33}$$

where the integral is taken along the cycle path, as presented in Figures 6, and respectively 7, left. The cycle net specific heat can be determined as [14]:

$$q_{cycle} = \oint T ds \tag{34}$$

where the integral is taken along the cycle path, as presented in Figures 6, and respectively 7, right. Finally, the cycle efficiency is [14]:

$$\eta_{cycle} = \frac{w_{cycle}}{q_{cycle}} \tag{35}$$

For the case presented herein, the resulting net work, net heat, and cycle efficiency for the three employed models are presented in Table 5.

Table 5: Net work, net heat and cycle efficiency

Model	Net specific work [J/kg]		Net specific heat [J/kg]		Cycle efficiency [%]	
	Ideal	Real	Ideal	Real	Ideal	Real
H	1879507.55	1691051.73	2319215.31	2089956.28	81.0406668	80.9132586
FJ	1948766.86	1764894.31	2632753.53	2391403.21	74.0201027	73.8016197
ZND	3543540.28	3166220.34	4569887.30	4086266.64	77.5410868	77.4844282

The highest cycle specific is provided by the Zeldovich - von Neumann - Doring cycle, while the highest efficiency is provided by the Humphrey model.

6 CONCLUSION

A review of the existing thermodynamic cycle models for detonation is presented. Based on this review, three such models are selected to provide basis for the computation of the TIDE engine thermodynamic cycle: the Humphrey cycle, the Zeldovitch - Neumann - van Doring cycle, and the Fickett - Jacobs cycle.
The algorithms for the computation of the real and ideal thermodynamic cycles for each models are next presented, followed by numerical results reflecting the conditions of the TIDE engine.
Finally, the net specific work and heat, as well as the cycle efficiencies of the TIDE engine according to each of the selected detonation model cycles are presented.
The the Zeldovitch - Neumann - van Doring cycle provides the highest work, of 3543.5 kJ / kg in the ideal case, and of 3166.2 kJ / kg in the real case, while the Humphrey cycle provides the highest efficiency, of 81.0 % in the ideal case, and of 80.9 % in the real case.

7 REFERENCES

1. R. Vutthivithayarak. Analysis of Pulse Detonation Tubojet Engines.PhD Thesis, University of Texas at Arlington, 2011.
2. W. H. Heiser and D. T. Pratt. Thermodynamic Cycle Analysis of Pulse Detonation Engines.Journal of Propulsion and Power, vol. 18, 2002.
3. V. Stanciu - "Motoare aeroreactoare (Indrumar de anteproiectare)". Institutul Politehnic Bucuresti. Facultatea de Aeronave. Bucuresti, Romania, 1992
4. S.R. Turns – "An introduction to combustion. Concept and applications". McGraw – Hill International Editions, 2000
5. V. Pimnsner - "Motoare aeroreactoare. Vol. I" Editura Didactica si Pedagogica, Bucuresti, 1983
6. E. Wintenberger, J.E. Shepherd, "Thermodynamic cycle analysis for propagating detonation", Journal of Propulsion and Power, vol. 22, no. 3, pp. 694 - 697, 2006
7. D.L. Chapman, "On the Rate of Explosion in Gases," Philosophical Magazine Series 5, vol. 47, no. 284, 1889, pp. 90–104.
8. H.A. Humphrey - "An Internal-Combustion Pump, and Other Applications of a New Principle", Proceedings of the Institute of Mechanical Engineers vol. 77, no. 1, pp. 1075 – 1200, 1909
9. W. Fickett, W.C. Davis - "Detonation Theory and Experiment", Dover Publications Inc., 2001
10. S.J. Jacobs - "The Energy of Detonation," NAVORD Report 4366, U.S. Naval Ordnance Laboratory, White Oak, MD, USA, 1956
11. Y.B. Zeldovich, "K Teori rasprostranenia detonazi v gasoobrasnikh systemakh", Zhurnal Experimentalnoi i Teoreticheskoi Fiziki, vol. 10, pp. 543–568, 1940
12. E. Jouguet, "Sur la propagation des reactions chimiques dans les gaz," Journal des Mathematiques Pures et Appliquees, vol. 1, no. 1905, pp. 347–425
13. E. Jouguet, "Sur la propagation des reactions chimiques dans les gaz," Journal des Mathematiques Pures et Appliquees, vol. 2, no. 1906, pp. 5–86
14. R. Vutthivithayarak, E.M. Braun, F.K. Lu, "Examination of the various cycles for pulse detonation engines", AIAA 2011-6064, 47th AIAA/ASME/SAE/ASEE Joint Propulsion Conference & Exhibit, San Diego, California, USA, 2011
15. R. Bellini, "Ideal Cycle Analysis of a Regenerative Pulse Cycle Detonation Engine for Power Production", Ph.D. Thesis, University of Texas, Arlington, TX. USA, 2010